



Validation of INSAT-3D sounder data with in situ measurements and other similar satellite observations over India

Madineni Venkat Ratnam, Alladi Hemanth Kumar, and Achuthan Jayaraman

National Atmospheric Research Laboratory, Gadanki, India

Correspondence to: M. Venkat Ratnam (vratnam@narl.gov.in)

Received: 7 June 2016 – Published in Atmos. Meas. Tech. Discuss.: 27 July 2016

Revised: 26 October 2016 – Accepted: 10 November 2016 – Published: 30 November 2016

Abstract. To date, several satellites measurements are available which can provide profiles of temperature and water vapour with reasonable accuracies. However, the temporal resolution has remained poor, particularly over the tropics, as most of them are polar orbiting. At this juncture, the launch of INSAT-3D (Indian National Satellite System) by the Indian Space Research Organization (ISRO) on 26 July 2013 carrying a multi-spectral imager covering visible to long-wave infrared made it possible to obtain profiles of temperature and water vapour over India with higher temporal and vertical resolutions and altitude coverage, besides other parameters. The initial validation of INSAT-3D data is made with the high temporal (3 h) resolution radiosonde observations launched over Gadanki (13.5° N, 79.2° E) during a special campaign and routine evening soundings obtained at 12:00 UTC (17:30 LT). We also compared INSAT-3D data with the radiosonde observations obtained from 34 India Meteorological Department stations. Comparisons were also made over India with data from other satellites like AIRS, MLS and SAPHIR and from ERA-Interim and NCEP reanalysis data sets. INSAT-3D is able to show better coverage over India with high spatial and temporal resolutions as expected. Good correlation in temperature between INSAT-3D and in situ measurements is noticed except in the upper tropospheric and lower stratospheric regions (positive bias of 2–3 K). There is a mean dry bias of 20–30% in the water vapour mixing ratio. Similar biases are noticed when compared to other satellites and reanalysis data sets. INSAT-3D shows a large positive bias in temperature above 25° N in the lower troposphere. Thus, caution is advised when using these data for tropospheric studies. Finally it is concluded that temperature data from INSAT-3D are of high quality and can be directly assimilated for better forecasts over India.

1 Introduction

Temperature and water vapour play an important role in deciding the thermodynamic state of the atmosphere as they are considered to be feedback parameters which alter the radiation and moist dynamics of the atmosphere. The stability of the earth's atmosphere (troposphere and stratosphere) depends on the density of the air parcel at any particular altitude. The density of the air parcel depends on the amount of water vapour present in it as well as its temperature. The water vapour is a highly varying parameter which is mainly responsible for precipitation and all other weather systems. It is the source of the latent heat which is released into the atmosphere during cloud formation. It also dominates the structure of diabatic heating of the earth's atmosphere (Trenberth et al., 2005; Trenberth and Stepaniak, 2003a, b). These parameters vary in time and as well as in space (both vertically and horizontally) throughout the atmosphere.

Profiles of temperature (T) and relative humidity (RH) or water vapour (WV) are traditionally obtained from the in situ conventional radiosonde measurements which have high vertical resolutions and accuracies. However, they have limited spatial and temporal coverage. For this reason, satellites are considered the best source of information for obtaining these parameters because they provide observations on a global scale with improved temporal resolution based on the orbit in which the satellite is present. Among several satellites, Atmospheric Infrared Sounder (AIRS), Microwave Limb Sounder (MLS) and GPS Radio Occultation provide profiles of temperature and water vapour with reasonable accuracies. The incomplete coverage of AIRS and MLS because of orbit gaps in the tropical regions can be overcome by geostationary sounders that have complete coverage over a given region. Recently Sounder for Atmospheric Profil-

ing of Humidity in the Inter-tropical Regions (SAPHIR) on board Megha-Tropiques has been introduced which provides profiles of RH in the tropical latitudes (Venkat Ratnam et al., 2013). They have good spatial coverage but the temporal resolution of these satellites is poor. At this juncture, the launch of the Indian National Satellite System (INSAT)-3D in July 2013 has gained lot of significance due to its geostationary transfer orbit which provides profiles of T and WV with high temporal resolutions. It is restricted to India unlike the satellites mentioned above. These data are expected to play an important role in numerical weather prediction over India. Before using these data for weather forecasting, it is essential to validate them with similar in situ satellite and reanalysis data sets.

In this report, we discussed the features of T and WV obtained from the INSAT-3D sounder. It adds a new dimension by providing continuous observations of T and WV over India, thereby monitoring the earth's weather systems continuously. In the first section we compared the broad features of T and WV obtained from INSAT-3D with the other satellite observations. This is followed by the validation of INSAT-3D data with a high-resolution radiosonde launched during a special campaign (tropical tropopause dynamics campaigns) (Venkat Ratnam et al., 2014b) and routine evening soundings over Gadanki (13.5° N, 79.2° E), a tropical station in the southern peninsular India. We also compared these data with the India Meteorological Department (IMD) network of radiosondes, consisting of 34 stations over India. In this context it is worth quoting Mitra et al. (2015), who compared INSAT-3D data obtained from January to May 2014 at 10 GPS stations of IMD. However, their work is restricted up to 100 hPa only and for the initial 5 months. In the present work we extended comparisons for 2 complete years (2014 and 2015) and up to 10 hPa. Further, the comparisons are also made with other satellite observations like AIRS (Atmospheric Infrared Sounder), Microwave Limb Sounder (MLS), and SAPHIR (Sounder for Atmospheric Profiling of Humidity in the Inter-tropical Regions) and reanalysis data sets like ERA-Interim (European Centre for Medium-Range Weather Forecasts, ECMWF) and the NCEP (National Center for Environmental Prediction).

2 Database

2.1 INSAT-3D

The INSAT-3D, which is considered to be the advanced version of all the other INSAT series satellites, is a meteorological satellite of ISRO launched from Kourou, French Guiana, as a passenger payload along with AlphaSat/InmarSat-I-XL, ESA/InmarSat by the European launch vehicle named Ariane-5 VA-214 on 26 July 2013. It was positioned at 82° E over the equator at an altitude of 35 786 km from the surface of earth in the geostationary transfer orbit (GTO) with

the main objectives of monitoring the earth and ocean continuously, thereby providing the data dissemination capabilities. It also provides an operational, environmental and storm warning system to protect lives and property. It carries four payloads, of which the multi-spectral imager and atmospheric sounder are of key importance. The multi-spectral imager (optical radiometer) provides high-resolution images of the mesoscale phenomena and local storms mainly in the visible band, apart from imaging the whole earth disk in the short-wave infrared, mid-infrared, water vapour and low thermal infrared channels. The atmospheric sounder, which has 19 channels in the short-wave infrared, mid-infrared, long-wave infrared (18) and visible (1) measures the irradiance and provides profiles of T , WV and integrated ozone over the selected land mass of India every hour and over the whole of the Indian Ocean every 6 h as shown in Table 1.

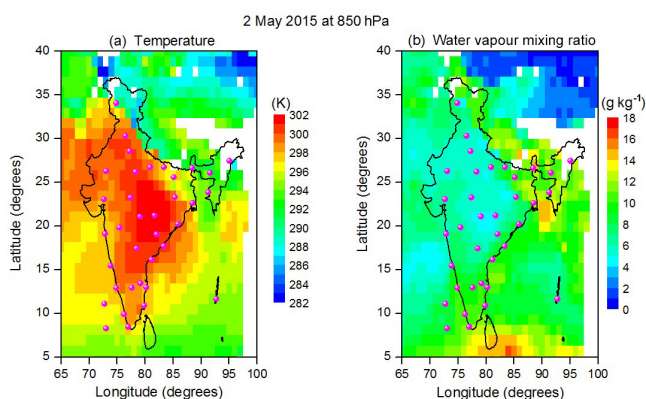
This atmospheric sounder gives profiles of T and WV at 40 pressure levels (1000, 950, 920, 850, 750, 700, 670, 620, 570, 500, 475, 430, 400, 350, 300, 250, 200, 150, 135, 115, 100, 85, 70, 60, 50, 30, 25, 20, 15, 10, 7, 5, 4, 3, 2, 1.5, 1, 0.5, 0.2, 0.1 hPa) every 1 h at 10 km \times 10 km in latitude and longitude resolutions covering 5–40° N and 60–100° E over India region. The INSAT-3D sounder provides T and WV profiles along with the total columnar ozone from the infrared radiances obtained in different absorption bands during the clear sky conditions. The retrieval algorithm adopted for INSAT-3D sounder is the same as that adopted for HIRS (High-resolution Infrared Radiation Sounder) and GOES (Geostationary Operational Environmental Satellite), which are mainly based on the retrieval algorithm of Hayden (1988), Ma et al. (1999) and Li et al. (2000). The INSAT-3D cloud mask algorithm builds on the basis of the algorithm adopted by Ackerman et al. (1998). In brief, a clear composite of the maximum brightness temperature (BT) in thermal channels is generated to get a rough idea about the surface temperature in the clear sky condition at a particular time. This will be the reference background temperature on which the threshold for a particular location will be determined to discriminate cloud. Several tests, such as the BT threshold test, difference test1 (BT11 – BT3.7), difference test2 (BT3.7 – BT12), spatial variability test, spatial uniformity test, adjacent pixel test, temporal uniformity test and final threshold test, are applied to each pixel to find out whether the pixel is cloudy, clear, partially cloudy or partially clear.

2.2 Radiosonde observations

The processed and quality-checked radiosonde data obtained from the Integrated Global Radiosonde Archive (Durre et al., 2006) over India at different locations (0–40° N, 60–100° E) during the period 2014–2015 are obtained. The observed unexpected sharp spikes in the data are removed and only the data values which are within the range $\pm 2\sigma$ in T and WV from the mean are considered for comparison. Such stringent quality-checked data are utilised for comparison with

Table 1. The principal absorbing gases of the infrared radiation in the atmosphere at different channels in INSAT-3D with their central wavelengths and their purpose of retrieval.

Detector	Ch. No.	Wavelength(μm)	Principal absorbing gas	Purpose
Long wave	1	14.67	CO ₂	Stratosphere temperature
	2	14.31	CO ₂	Tropopause temperature
	3	14.03	CO ₂	Upper-level temperature
	4	13.64	CO ₂	Mid-level temperature
	5	13.33	CO ₂	Low-level temperature
	6	12.59	Water vapour	Total precipitable water
Medium wave	7	11.98	Water vapour	Surface temperature, moisture
	8	10.99	Window	Surface temperature
	9	9.69	Ozone	Total ozone
	10	7.43	Water vapour	Low-level moisture
	11	7.04	Water vapour	Mid-level moisture
	12	6.52	Water vapour	Upper-level moisture
Short wave	13	4.61	N ₂ O	Low-level temperature
	14	4.54	N ₂ O	Mid-level temperature
	15	4.48	CO ₂	Upper-level temperature
	16	4.15	CO ₂	Boundary-level temperature
	17	4.01	Window	Surface temperature
	18	3.79	Window	Surface temperature, moisture

**Figure 1.** Spatial variation of (a) temperature and (b) water vapour mixing ratio over India at 850 hPa pressure level obtained from INSAT-3D satellite on 2 May 2015 (averaged over a day). The filled circles (magenta) in both panels show the locations of IMD radiosonde stations selected within 0–40° N latitude and 60–100° E longitude (India) for comparing INSAT-3D observations. White patches show the non-availability of the data.

the T and WV obtained from INSAT-3D. The 34 locations of the radiosonde stations over India (i.e. IMD stations) are shown in the Fig. 1. The data from these IMD stations obtained at 00:00 UTC (05:30 LT) are only used for comparison as the 12:00 UTC (17:30 LT) data during this period are very sparse.

Further, high vertical resolution GPS radiosondes (Meisei RS-11 G, Japan) that were launched over Gadanki around 12:00 UTC (17:30 LT) are used in the present study. Besides

these routine evening radiosonde launches, the radiosondes that were launched as a part of a special campaign between January and March 2014 over the same location are also utilised for comparison at subdaily scales. The sensors used for measuring the T and WV are thermistors and carbon hygrometers, respectively. The range of the T and relative humidity (RH) measured by the sensors are -90 to $+50$ °C and 1–100 % with accuracies of 0.5 K and 5–7 %, respectively (Basha and Venkat Ratnam, 2009; Venkat Ratnam et al., 2014a). During this campaign the radiosondes were launched every 3 h (11:30, 14:30, 17:30, 20:30, 23:30, 02:30, 05:30 and 08:30 IST) for three consecutive days. The entirety of the radiosonde data sets are interpolated to the pressure levels of INSAT-3D data. The INSAT-3D data available within $\pm 1^\circ$ latitude and longitude from a given station and within ± 1 h are used for comparison.

2.3 Other satellite observations

2.3.1 AIRS observations

AIRS is one of the payloads on the NASA Earth Observing System satellite, AQUA, which is in a polar sun synchronous orbit, revolving at an altitude of 705 km from the earth's surface with an orbital period of 98.99 min. It completes approximately 14.5 orbits per day and the separation between any two consecutive orbits near the equator is 2760 km. The partner payloads along with AIRS on board the AQUA satellite are the microwave instruments AMSU and the Humidity Sounder for Brazil. The satellite crosses the equator twice a day, once during the ascending node at $\sim 13:30$ LT and once

during the descending node at $\sim 01:30$ LT. It is a high spectral sounder with 2378 channels measuring the IR radiances at wavelengths in the range of 3.7–15.4 μm with a swath of 1650 km and horizontal spatial resolution of 13.5 km at nadir (Aumann et al., 2003). We used the level 3 version 5 daily gridded data products (Susskind et al., 2006) obtained from the IR radiances of the AIRS sounder during 2014 and 2015. The level 3 data products (AIRS V5 L3) are obtained from the level 2 swath data, in which the data from all 15 orbits of the day are averaged together and the data have a latitudinal and longitudinal resolution of $1^\circ \times 1^\circ$ at 24 pressure levels for T from 1000 to 1 hPa and 12 levels for WV from 1000 to 100 hPa. Note that WV data are reliable in the first 8 levels from the surface and up to 300 hPa (Waters et al., 2006).

2.3.2 MLS observations

MLS is one of the four payloads on board NASA's EOS Aura satellite which is one among the six satellites (OCO-2, GCOM-W1, AQUA, CLOUDSAT, CALIPSO, AURA) that form the A-Train constellation. Similarly to AIRS, MLS is a polar-orbiting sun synchronous satellite (AURA) at ~ 705 km, scanning its view from the ground to ~ 90 km at 55 pressure levels with a global view covering 82° S to 82° N by having ~ 15 orbits per day. It scans the earth's atmosphere every 25 s and provides 240 scans per orbit. The details regarding the MLS measurement technique and instrumentation are discussed by Waters et al. (2006). The MLS measures the thermal emission of the earth through its limb-viewing geometry at a microwave band centred near 118, 190, 240, 640 and 2500 GHz and its retrieval algorithm can be found from Livesey et al. (2006). We made use of the level 2 version 3 temperature and water vapour data during the period 2014 and 2015 which were downloaded from <http://mirador.gsfc.nasa.gov>. Note that water vapour from this instrument is more valid above 300 hPa (Basha et al., 2013).

2.3.3 SAPHIR observations

SAPHIR is one of the four instruments on board the Megha-Tropiques (MT) satellite and moves in a circular low-inclination orbit at 20° with 14 orbits per day. It provides a cross-track scan of $\pm 43^\circ$ with a swath of 1705 km and resolution of 10 km at nadir. It is a passive remote-sensing microwave sounder which operates at six channels close to 183.31 GHz (± 11.0 , ± 6.60 , ± 4.30 , ± 2.8 , ± 1.2), retrieving layer-averaged RH values in six pressure layers (1000–850, 850–700, 700–550, 550–400, 400–250 and 250–100 hPa) within $\pm 30^\circ$ latitudinal belt. The algorithms related to retrieval for the sounders of the MT satellite are discussed by Gohil et al. (2012). These data have been validated against similar satellites and reanalysis data sets and found to be good except in level 1 (1000–850 hPa) (Venkat Ratnam et al., 2013). For comparison, we made use of the SAPHIR RH

data, which were downloaded from www.mosdac.gov.in for the period 2014–2015. Note that RH is available from this satellite but WV mixing ratio is not.

2.4 Reanalysis data sets

2.4.1 ERA-Interim data

ERA-Interim is the advanced global atmospheric reanalysis produced by ECMWF. It provides gridded data products which include large surface parameters every 3 h and upper-air parameters covering the troposphere and stratosphere every 6 h from 1979 onwards. The data products are obtained from the model through a sequential data assimilation method in which the models are fed with the available observations to forecast the evolving state of the global atmosphere. The configuration and performance of the ERA-Interim reanalysis are explained clearly by Dee et al. (2011). It is even considered the latest and most advanced global assimilation scheme and can predict the atmosphere to the nearest possible accuracy (Simmons and Hollingsworth, 2002). These data products are available across the entire globe at different latitude and longitude resolutions and for 37 pressure levels from 1000 to 1 hPa. We have made use of $1^\circ \times 1^\circ$ data products of T and WV for the period 2014–2015.

2.4.2 NCEP/NCAR data

This data set is a joint product of National Centers for Environmental Prediction (NCEP) and National Center for Atmospheric Research (NCAR). Similarly to ERA-Interim, they provide gridded data which is available from 1948 onwards. NCEP data represent the state of the earth's atmosphere by incorporating the global historical observations and the output of the global numerical weather prediction (NWP) model (Kalnay et al., 1996). These data products are available all over the globe at $2.5^\circ \times 2.5^\circ$ latitude–longitude resolution at 17 pressure levels from 1000 to 10 hPa for temperature and eight pressure levels for WV from 1000 to 300 hPa. We made use of these data for T and WV during the period 2014–2015.

3 Results and discussion

In this section, observations from the advanced ISRO geostationary INSAT-3D satellite sounder, which provides continuous observations over the land and ocean of India, are discussed as they are very important in weather forecasting. The continuous observations of the sounder are very important as they can be introduced and combined with model output for a better forecast of the earth's atmosphere. Before they are used for any scientific purpose, it is essential to compare/validate them with similar data sets. Figure 1 shows the spatial variation of T and WV mixing ratio (WVMR) over India at 850 hPa pressure level obtained from INSAT-3D satellite on 2 May 2015 (averaged over a day). White patches

show the non-availability of data due to topography (the Himalayas). Higher temperatures of about 5–6 K over the main land mass compared to the surrounding sea can be noticed. On the contrary, there are very low values of WVMR over the land mass compared to the surrounding ocean.

The simultaneous observations from MLS and AIRS over India obtained around 13:30 IST (i.e. ascending node for AIRS and MLS) on the same day are considered for comparison. Spatial variation of T and WVMR over India observed at 500 hPa pressure level from INSAT-3D, MLS and AIRS satellites on 2 May 2015 around 13:30 IST is shown in Fig. 2. Spatial variation of T and WVMR over India obtained from ERA-Interim and NCEP at the same pressure level at 06:00 UTC (11:30 IST) is also shown. Although major features in the spatial variation of T are generally alike for different satellites and reanalysis data sets, a large difference in the WVMR can be noticed. In particular, AIRS shows large WVMR variations over the Bay of Bengal (BoB) and Himalayas compared to the other two satellites. Similarly high variation in WVMR is also seen by ERA-Interim (Fig. 2i). Very low WVMR values in central India and to the west in all the satellite observations can be noticed. The quantitative difference between INSAT-3D and other satellite measurements and reanalysis data sets will be discussed in later sections.

3.1 Comparison of INSAT-3D and radiosonde observations at subdaily scales

The INSAT-3D sounder provides profiles of T and WV over India almost every hour. It is desirable to compare these profiles at different times of the day, which is difficult to do with existing polar satellites. Thus, we compared the INSAT-3D profiles of T and WV with radiosonde observations obtained over Gadanki using the IMD network of radiosondes. It is well known that the most common and widespread in situ instruments for providing accurate profiles of T and WV are radiosondes, and these are typically employed for satellite sounder validation (e.g. Fetzer et al., 2003; Xie et al., 2013; Nalli et al., 2013). However, obtaining accurate measurements of WV with radiosondes in the upper troposphere and lower stratosphere, where the concentration of water vapour is very low, is a challenging task. In addition to this there is a radiation error in the temperature measurements as explained by Luers and Eskridge (1998) and Wang et al. (2003). We have used high accuracy and vertical resolution radiosonde over Gadanki, which were launched every 3 h for three consecutive days during a special campaign called tropical tropopause dynamics campaign (TTD) (Venkat Ratnam et al., 2014b) conducted over Gadanki between January and March 2014. These data are used to validate the INSAT-3D measurements at subdaily scales.

The radiosonde data obtained during the TTD campaigns are interpolated to the pressure levels of INSAT-3D for the similar hours whenever observations are available. Although Nalli et al. (2013) have pointed out the importance

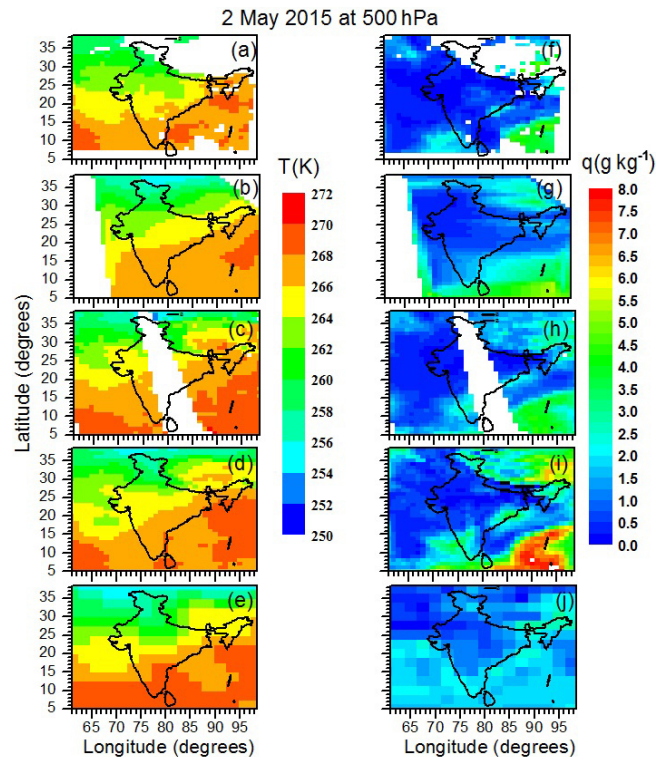


Figure 2. Spatial variation of temperature over India at 500 hPa pressure level obtained from (a) INSAT-3D, (b) MLS, (c) AIRS, (d) ERA-Interim and (e) NCEP on 2 May 2015 around 13:30 IST. (f)–(j) same as (a) to (e) but for water vapour mixing ratio. White patches show the non-availability of the data.

of a proper reduction of high vertical resolution radiosonde data to forward model layers, in the present study only the Gadanki radiosonde measurements are of high resolution. Thus, to maintain uniformity, we have retained the same analysis procedure as was done in our earlier study (Venkat Ratnam et al., 2013), including simple vertical interpolation of the radiosonde data. Typical temporal variation of T and WVMR obtained from radiosonde launched over Gadanki during one of the TTD campaigns conducted from 25 to 28 March 2014 is shown in Fig. 3. Data obtained from INSAT-3D at similar times are also shown in the bottom panels. In general, similar diurnal variation in the T and WVMR between radiosonde and INSAT-3D can be noticed, though the magnitude differs. Very cold temperatures (~ 190 K) present near the tropopause region (100 hPa) are captured well by INSAT-3D. The existence of high WVMR at night-time is also captured well by the INSAT-3D. The T and WVMR over Gadanki obtained from INSAT-3D and radiosonde are averaged over 3 days and the mean and standard deviation are shown in Fig. 3e and f, respectively. From these profiles, no significant difference in the T can be noticed but there is an underestimation of WVMR by INSAT-3D (assuming radiosonde as standard technique). INSAT-3D shows

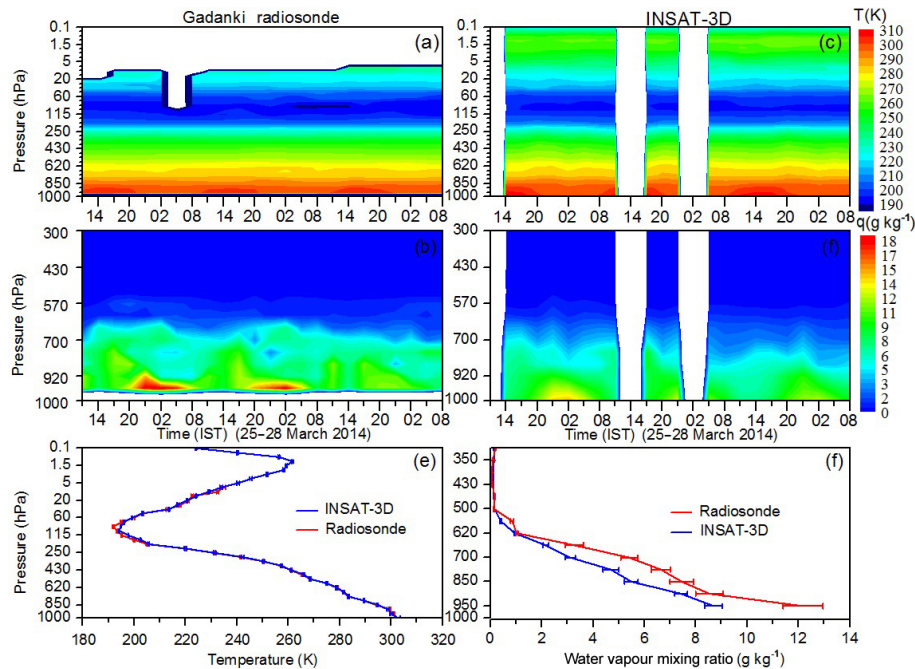


Figure 3. Temporal variation of (a) temperature and (b) water vapour mixing ratio obtained from radiosonde launched over Gadanki during the TTD campaign conducted from 25 to 28 March 2014. White patches show the non-availability of the data. Panels (c) and (d) are the same as (a) and (b) but observed by INSAT-3D. The mean profiles of (e) temperature and (f) water vapour mixing ratio obtained from radiosonde (red) and INSAT-3D (blue). Horizontal lines indicate standard deviations.

a dry bias of $3\text{--}4\text{ g kg}^{-1}$ in WVMR when compared to radiosonde observations. No significant day–night differences are noticed between the INSAT-3D and Gadanki radiosonde observations.

3.2 Comparison of INSAT-3D and radiosonde (IMD and Gadanki) observations

We also compared INSAT-3D measurements obtained during 2014 and 2015 with the radiosonde observations from the 34 IMD stations, which are spread throughout India and are shown in the form of filled circles in Fig. 1. Besides these, the routine evening radiosonde observations launched around 12:00 UTC (17:30 LT) over Gadanki during 2014–2015 were utilised for day-to-day comparisons. The radiosonde data of all the IMD stations are interpolated to the pressure levels of INSAT-3D for uniformity. The correlation coefficient values obtained for T and RH (WVMR is not available directly from IMD data) between the INSAT-3D and Gadanki radiosondes launched around 12:00 UTC (17:30 LT) and IMD radiosonde launched around 00:00 UTC (05:30 LT) over India are obtained separately for each day during the period 2014–2015. Note that both T and WV information is used for estimating RH. The correlation values are obtained for all the levels in T but only up to 300 hPa (as RH obtained from radiosonde is not accurate above -40°C or $\sim 12\text{ km}$. Beyond this altitude the radiosonde humidity sensors are not sensitive) in RH and is shown in Fig. 4. A very high corre-

lation (>0.8) in T between INSAT-3D and IMD/Gadanki radiosonde is observed in the lower troposphere (Fig. 4a). However, correlation decreases above 700 hPa (850 hPa) between INSAT-3D and Gadanki (IMD) radiosonde. There is a consistent correlation of more than 0.6 throughout all levels with the Gadanki radiosonde but it drastically decreases above 250 hPa in the case of IMD radiosondes. It is interesting to notice higher (lower) correlation below (above) 850 hPa between Gadanki radiosonde and INSAT-3D. However, the opposite is found in the case of IMD radiosonde, the reason for which is not known. The correlation values of RH obtained between the INSAT-3D and Gadanki radiosondes is always higher (greater than 0.65) throughout the profile than the correlation obtained between INSAT-3D and IMD radiosonde observations (less than 0.5) shown Fig. 4b. Mitra et al. (2015) have reported similar correlations using 10 IMD stations using 5 months (January–May 2014) of the data. However, their work is restricted up to 100 hPa due to frequent balloon bursts of IMD radiosondes at that altitude. In the present study we report up to 10 hPa using 2 complete years of the data for Gadanki. The observed good correlation (0.6–0.7) between INSAT-3D RH and Gadanki RH may be attributed to the improved sensor used in Meisei radiosondes which were used over Gadanki.

Further, to quantify the differences between the INSAT-3D and Gadanki radiosondes, we discuss the fractional difference at all levels between routine radiosondes launched

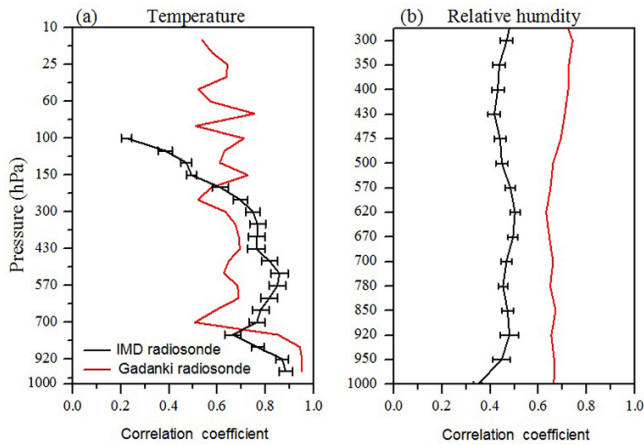


Figure 4. Correlation coefficients obtained in (a) temperature and (b) relative humidity at different pressure levels between INSAT-3D and 12:00 UTC (17:30 LT) Gadanki radiosondes (red line) and 00:00 UTC (05:30 LT) IMD radiosondes (black line). Horizontal bars show the deviations in correlation coefficients obtained from 34 stations. Note that correlation coefficient up to 300 hPa is only obtained for relative humidity.

around 12:00 UTC over Gadanki and INSAT-3D T over the same site during the period 2014–2015. The fractional difference of T for each day is calculated separately, then averaged over 2014–2015. The balloon bursting altitude of the radiosonde is also estimated for those which are utilised in estimating the fractional difference. The fractional difference of T and RH and the balloon bursting altitude are shown in Fig. 5. It is clear from the figure that the difference is much smaller in the troposphere (~ 0.5 K). The mean fractional difference in the troposphere is less than 0.5 K, and it is about 1 K in the upper troposphere and lower stratosphere. However, a positive bias (INSAT-3D showing higher temperatures) of 2–3 K is noticed in day-to-day differences in INSAT-3D. When we segregated fractional differences by season, a higher fractional difference during monsoon season is noticed (figure not shown), mainly due to a fewer number of matches between the INSAT-3D and Gadanki radiosondes due to overcast conditions. The most striking feature is the consistent positive bias of 1% (~ 2 K) in T in the upper troposphere and lower stratosphere. The mean fractional difference in RH shown in Fig. 5b reveals a 20–30% dry bias in INSAT-3D compared to radiosonde. A dry bias of 40–60% is found in day-to-day comparisons of RH between INSAT-3D and the radiosonde. Thus, from Fig. 5, it is clear that INSAT-3D is able to provide T measurements with high accuracies but a huge dry bias is observed in RH. Thus, caution is advised while using RH data from INSAT-3D.

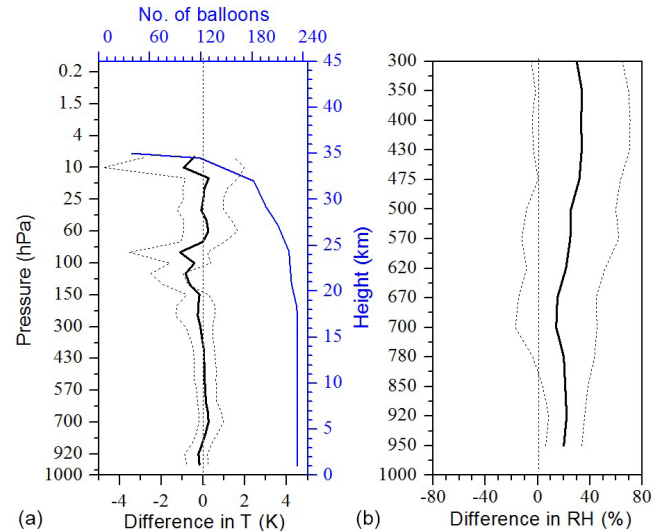


Figure 5. Fractional mean difference (thick line) and standard deviation (dotted lines) observed in the (a) temperature and (b) relative humidity between the INSAT-3D and Gadanki radiosondes launched at around 12:00 UTC (17:30 LT) over Gadanki during 2014–2015. The blue line in (a) represents the number of radiosondes reaching different altitudes (top-right axis).

3.3 Comparison of INSAT-3D and other satellite and reanalysis data

The T and WVMR retrieved from the radiances of 19 channels of the INSAT-3D sounder are compared with those obtained from other satellites like AIRS, MLS and SAPHIR (only RH) during the period 2014–2015. Besides the satellite observations, reanalysis data sets like ERA-Interim and NCEP are also utilised for comparing the data obtained from INSAT-3D. The T measurements obtained from AIRS, MLS and ERA-Interim are converted to a spatial resolution of $1^\circ \times 1^\circ$ in latitude and longitude. The $1^\circ \times 1^\circ$ gridded AIRS and MLS T measurements are interpolated to 40 pressure levels of INSAT-3D. However, the INSAT-3D data are converted to a spatial resolution of $2.5^\circ \times 2.5^\circ$ so they can be compared with the T obtained from NCEP. The difference in T between INSAT-3D, AIRS and MLS is estimated for each day whereas it is estimated every 6 h between INSAT-3D, ERA-Interim and NCEP. The zonal mean latitudinal difference of T between different satellites and reanalysis data sets is obtained for each day and then averaged for 2014 and 2015, which is shown in Fig. 6. In general, the difference in T between INSAT-3D and other satellite and reanalysis data sets lies within ± 1 K and extends to 2 K in the UTLS region. Above 25° N, INSAT-3D shows a positive bias of more than 4 K up to 300 hPa compared to AIRS but up to 700 hPa with the rest of the data sets. A consistent positive bias of 2–3 K in the UTLS region can be noticed in INSAT-3D, particularly compared with other satellite measurements. Above 4 hPa, a consistent negative bias of more than 3 K is

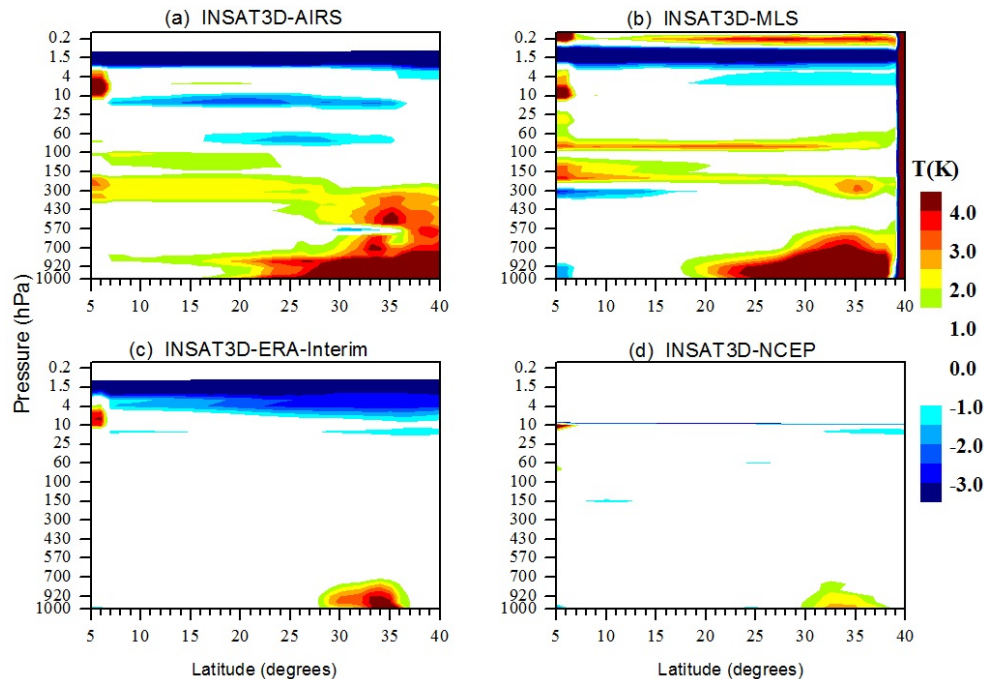


Figure 6. Zonal mean latitudinal difference between the INSAT-3D temperature and (a) AIRS, (b) MLS, (c) ERA-Interim and (d) NCEP temperatures observed during 2014–2015. The contours with differences within 1 K are omitted.

noticed in INSAT-3D compared to other data sets. In general, a smaller difference is noticed between INSAT-3D and NCEP than in ERA-Interim. Thus, the difference in T between INSAT-3D and other data sets is smallest in the lower and mid-troposphere below 25° N, whereas it increases in the lower troposphere above 25° N.

The WVMR data obtained from AIRS, MLS, ERA-Interim are converted to a spatial resolution of $1^{\circ} \times 1^{\circ}$ in latitude and longitude and then interpolated to the first 21 pressure levels of INSAT-3D. To compare the INSAT-3D WVMR data with NCEP WVMR data, the WVMR data obtained from INSAT-3D is converted to the actual resolution of NCEP, i.e. $2.5^{\circ} \times 2.5^{\circ}$ latitude and longitude grids. Note that information on WVMR data obtained from NCEP is only present up to 300 hPa, MLS from 300 hPa and above, whereas WVMR from AIRS and ERA-Interim is considered up to 100 hPa, beyond which the concentration of water vapour is very low. However, the RH obtained from SAPHIR in the troposphere is measured as layer-averaged relative humidity at certain levels as mentioned in Sect. 2. In order to compare the INSAT-3D RH data with SAPHIR RH, the former is converted to the pressure levels of SAPHIR. The zonal mean latitudinal difference between INSAT-3D and all other data sets is obtained as mentioned in the previous section and is presented in Fig. 7. In general, INSAT-3D shows a dry bias of 5–10% in the lower and mid-troposphere below 25° N when compared with AIRS (Fig. 7a), ERA-Interim (Fig. 7c) and NCEP (Fig. 7d) reanalysis data sets. However,

it shows a dry bias of more than 10% when compared with MLS (Fig. 7b). Note that INSAT-3D also shows a wet bias around 700 hPa with all the data sets. A high dry bias in the lower troposphere above 25° N is observed between INSAT-3D and AIRS, ERA-Interim and NCEP, whereas the bias in the same region is lower with MLS. The wet bias ($\sim 20\%$) between INSAT-3D and AIRS above 300 hPa is mainly due to low accuracies of AIRS at those altitudes (Waters et al., 2006). There is a dry bias of 20% between INSAT-3D and SAPHIR in the first two layers but it is reduced to less than 10% above (Fig. 7e). In this context it is worth quoting findings of Venkat Ratnam et al. (2013), who reported that the first layer (1000–850 hPa) of SAPHIR has large difference when compared to similar satellites. Thus, the present result of a large difference between INSAT-3D and SAPHIR in the lower most layers is expected. Note that no data are present in SAPHIR above 27° due to its low inclination.

4 Consistency check of T measurements of INSAT-3D in the UTLS region

From the previous section, it is clear that INSAT-3D overestimates T by 1% in the UTLS region. However, in order to check whether this positive bias is consistent or not, we compared the tropopause temperature obtained from radiosondes. The cold point tropopause temperature (CPT), which is the minimum in the temperature profile below 20 km, is obtained from radiosondes and INSAT-3D for each day dur-

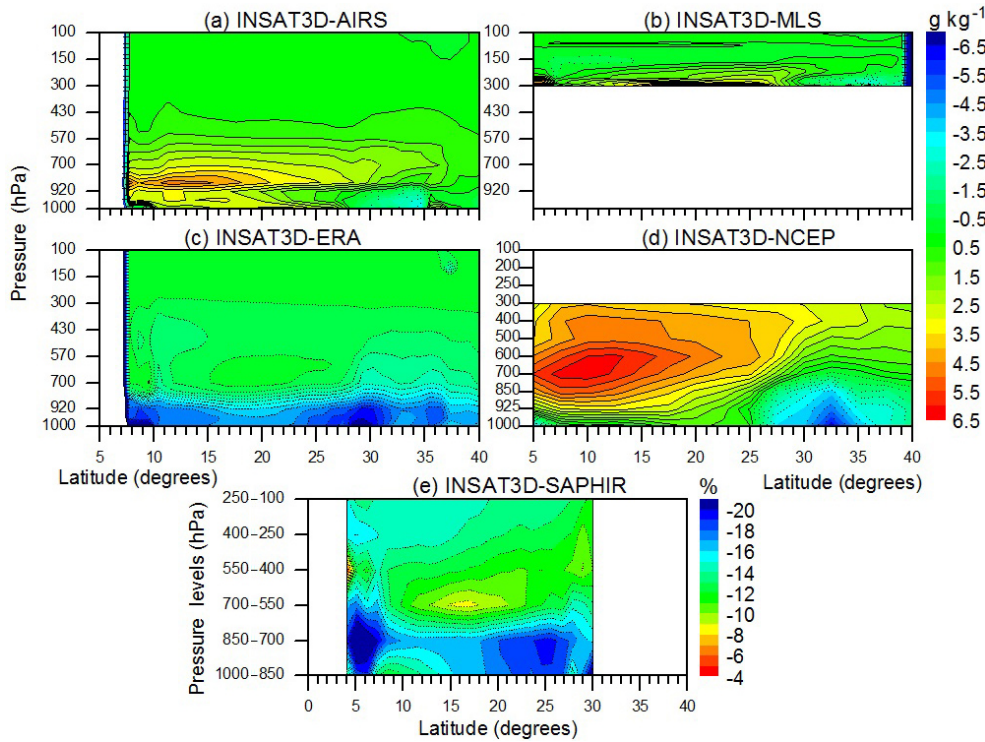


Figure 7. Zonal mean latitudinal difference between the INSAT-3D WVMR and (a) AIRS WVMR, (b) MLS WVMR, (c) ERA-Interim WVMR, (d) NCEP WVMR and (e) SAPHIR RH observed during 2014–2015. White patches show the non-availability of the data. The dotted (thick) line contours show the negative (positive) differences between INSAT-3D and the respective data sets.

ing 2014–2015 and is shown in Fig. 8. A consistent positive bias of 2–3 K is seen in CPT between the INSAT-3D and Gadanki radiosondes as expected; however, general trends match well between the two. The CPT obtained from INSAT-3D matches well with the radiosonde observations and shows a clear annual variability with higher values during the summer monsoon months (JJA) and lower values observed in winter months (DJF). This seasonal variability of the CPT over India during different seasons is consistent with reports by Mehta et al. (2010). These results are also consistent with earlier reports over other regions at tropical latitude (Newell et al., 1969; Reed and Vlcek, 1969; Reid and Gage, 1996; Seidel et al., 2001) in which it was attributed to the annual modulation of the Hadley cell. Thus, INSAT-3D data can be effectively utilised to investigate the tropopause characteristics to verify the new features reported in Venkat Ratnam et al. (2005), but with a known caution of overestimation of T by 2–3 K. As the data from INSAT-3D are available for almost every hour, they are very useful for investigating stratosphere–troposphere exchange (STE) process occurring at subdaily scales.

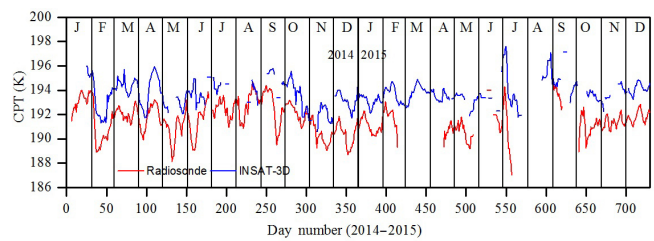


Figure 8. Time series of cold point tropopause temperatures (CPT) observed over Gadanki during 2014 and 2015 by INSAT-3D (blue line) and radiosonde (red line) at 12:00 UTC (17:30 LT). These are the 5-point running averages of CPT.

5 Summary and conclusions

The quality of the new data product, mainly the temperature (T) and water vapour (WV) obtained from the sounder payload on board INSAT-3D, is discussed. A detailed comparison of the data (T and WV) obtained from INSAT-3D with the existing in situ radiosonde measurements over the whole of India, similar satellite (AIRS, MLS and SAPHIR) observations and reanalysis (ERA-Interim and NCEP) data sets has been carried out in the present study. The main conclusions drawn from the study are as follows.

INSAT-3D provides measurements with very good spatial and temporal coverage over India compared to any other satellites, as is expected.

INSAT-3D is able to measure the general features of temperature and water vapour similar to the radiosonde observations even at subdaily scales. However, magnitudes differ (are underestimated) in water vapour measured by INSAT-3D. There is no day–night difference in the temperature measurements of INSAT-3D.

The mean difference between INSAT-3D and radiosonde temperature in the troposphere is less than 0.5 K with standard deviations of 1 K. However, mean difference in water vapour is as high as 20–30 % with standard deviations of 40–60 %.

The RH values obtained from INSAT-3D are better correlated ($R^2 = 0.6–0.7$) with the Gadanki radiosonde RH than the IMD radiosonde ($R^2 < 0.5$) due to the improved sensor.

There is a consistent positive bias ($\sim 2–3$ K) in temperature in the upper troposphere and lower stratosphere in INSAT-3D.

A dry bias of 10–25 % in the INSAT-3D measured water vapour compared to similar satellites and reanalysis data sets is noticed.

In general, temperature from INSAT-3D agrees well with all the other satellite measurements and reanalysis data sets below 25° N, whereas a difference of ~ 4 K in temperature above 25° N is noticed. INSAT-3D shows less temperature difference around tropopause region with AIRS and ERA-Interim data sets.

It is found that there is a large difference between INSAT-3D and other data sets both in temperature and water vapour above 25° N latitude perhaps due to their geometry. Thus, caution is advised when using INSAT-3D data over those locations. It is important to note that INSAT-3D shows good agreement with the conventional in situ radiosonde observations of both Gadanki and IMD locations over India, showing signs of good reliability to use the former data sets for measuring the temperature and water vapour spatially and temporally. A very small difference in temperature between INSAT-3D and radiosonde observations provides scope to use the INSAT-3D data in the numerical weather models for better forecasts. However, caution is again advised while using the water vapour because most of the time a mean dry bias of 20–30 % is noticed. Though consistent positive bias of $\sim 2–3$ K is observed in the cold point tropopause temperatures, the variability in the tropopause obtained from INSAT-3D shows an excellent match with the in situ radiosonde observations during 2014–2015. Thus, INSAT-3D data can also be used to study the tropopause characteristics at subdaily scales, which is not possible with any existing satellites or for stratosphere–troposphere exchange processes.

6 Data availability

The INSAT-3D data are available in the public domain from the portal www.mosdac.gov.in.

Acknowledgements. The INSAT-3D data used in the present study obtained from MOSDAC are greatly acknowledged. We thank AIRS, MLS, ERA-Interim and NCEP teams for providing data through their ftp sites. We thank the editor, one anonymous reviewer and J. M. Blaisdell for their constructive comments/suggestions which improved the manuscript content significantly.

Edited by: B. Kahn

Reviewed by: J. M. Blaisdell and one anonymous referee

References

- Ackerman, S. A., Strabala, K. I., Menzel, W. P., Frey, R. A., Moeller, C. C., and Gumley, L. E.: Discriminating clear sky from clouds with MODIS, *J. Geophys. Res.*, 103, 32141–32157, 1998.
- Ackerman, S. A., Strabala, K. I., Menzel, W. P., Frey, R. A., Moeller, C. C., and Gumley, L. E.: AIRS/AMSU/HSB on the Aqua mission: Design, science objectives, data products and processing system, *IEEE T. Geosci. Remote*, 41, 253–264, 2003.
- Basha, G. and Venkat Ratnam, M.: Identification of atmospheric boundary layer height over a tropical station using high resolution radiosonde refractivity profiles: Comparison with GPS radio occultation measurements, *J. Geophys. Res.*, 114, D16101, doi:10.1029/2008JD011692, 2009.
- Basha, G., Venkat Ratnam, M., and Krishna Murthy, B. V.: Upper tropospheric water vapour variability over tropical latitudes observed using radiosonde and satellite measurements, *Article, J. Earth Sys. Sci.*, 122, 1583–1591, 2013.
- Dee, D. P., Uppala, S. M., Simmons, A. J., Berrisford, P., Poli, P., Kobayashi, S., Andrae, U., Balmaseda, M. A., Balsamo, G., Bauer, P., Bechtold, P., Beljaars, A. C. M., van de Berg, L., Bidlot, J., Bormann, N., Delsol, C., Dragani, R., Fuentes, M., Geer, A. J., Haimberger, L., Healy, S. B., Hersbach, H., Holm, E. V., Isaksen, I., Kållberg, P., Kohler, M., Matricardi, M., McNally, A. P., Monge-Sanz, B. M., Morcrette, J.-J., Park, B.-K., Peubey, C., de Rosnay, P., Tavolato, C., Thepaut, J. N., and Vitart, F.: The ERA-Interim reanalysis: configuration and performance of the data assimilation system, *Q. J. Roy. Meteor. Soc.*, 137, 553–597, 2011.
- Durre, I., Vose, R., and Wuertz, D.: Overview of the Integrated Global Radiosonde Archive, *J. Climate*, 19, 53–68, 2006.
- Fetzer, E., McMillin, L. M., Tobin, D., Aumann, H. H., Gunson, M. R., McMillan, W. W., Hagan, D. E., Hofstadter, M. D., Yoe, J., Whiteman, D. N., Barnes, J. E., Bennartz, R., Vomel, H., Walden, V., Newchurch, M., Minnett, P. J., Atlas, R., Schmidlin, F., Olsen, E. T., Goldberg, M. D., Zhou, S., Ding, H., Smith, W. L., and Revercomb, H.: AIRS/AMSU/HSB validation, *IEEE T. Geosci. Remote*, 41, 418–431, 2003.
- Gohil, B. S., Gairola, R. M., Mathur, A. K., Varma, A. K., Mahesh, C., Gangwar, R. K., and Pal, P. K.: Algorithms for retrieving geophysical parameters from the MADRAS and SAPHIR sensors of the Megha-Tropiques satellite: Indian scenario, *Q. J. Roy. Meteor. Soc.*, 139, 954–963, doi:10.1002/qj.2041, 2012.

- Hayden, C. M.: GOES-VAS simultaneous temperature-moisture retrieval algorithm, *J. Appl. Meteor.*, 27, 705–733, 1988.
- Kalnay, E., Kanamitsu, M., Kistler, R., Collins, W., Deaven, D., Gandin, L., Iredell, M., Saha, S., White, G., Woollen, J., Zhu, Y., Chelliah, M., Ebisuzaki, W., Higgins, W., Janowiak, J., Mo, K. C., Ropelewski, C., Wang, J., Leetmaa, A., Reynolds, R., Jenne, R., and Joseph, D.: The NCEP/NCAR 40-year reanalysis project, *B. Am. Meteorol. Soc.*, 7, 437–471, 1996.
- Li, J. and Huang, H. L.: Retrieval of atmospheric profiles from satellite sounder measurements by use of the discrepancy principle, *Appl. Optics*, 38, 916–923, 1999.
- Li, J., Wolf, W. W., Menzel, W. P., Zhang, W., Huang, H. L., and Achtor, T. H.: Global soundings of the atmosphere from ATOVS measurements: The algorithm and validation, *J. Appl. Meteorol.*, 39, 1248–1268, 2000.
- Livesey, N. J., Snyder, W. V., Read, W. G., and Wagner, P. A.: Retrieval algorithms for the EOS Microwave Limb Sounder (MLS) instrument, *IEEE T. Geosci. Remote*, 44, 1144–1155, doi:10.1109/TGRS.2006.872327, 2006.
- Luers, J. K. and Eskridge, R. E.: Use of radiosonde temperature data in climate studies, *J. Climate*, 11, 1002–1019, 1998.
- Ma, X. L., Schmit, T., and Smith, W.: A non-linear physical retrieval algorithm – Its application to the GOES-8/9 sounder, *J. Appl. Meteor.*, 38, 501–503, 1999.
- Mehta, S. K., Venkat Ratnam, M., and Krishna Murthy, B. V.: Variability of the tropical tropopause over Indian monsoon region, *J. Geophys. Res.*, 115, D14120, doi:10.1029/2009JD012655, 2010.
- Mitra, A., Bhan, S., Sharma, A., Kaushik, N., Parihar, S., Mahandru, R., and Kundu, P. K.: INSAT-3D vertical profile retrievals at IMDPS, New Delhi, *Mausam*, 66, 687–694, 2015.
- Nalli, N. R., Barnet, C. D., Reale, A., Tobin, D., Gambacorta, A., Maddy, E. S., Joseph, E., Sun, B., Borg, L., Mollner, A. K., Morris, V. R., Liu, X., Divakarla, M., Minnett, P. J., Knuteson, R. O., King, T. S., and Wolf, W. W.: Validation of satellite sounder environmental data records: Application to the Cross-track Infrared Microwave Sounder Suite, *J. Geophys. Res.-Atmos.*, 118, 1–16, doi:10.1002/2013JD020436, 2013.
- Newell, R. E., Kidson, J. W., and Vincent, D. G.: Annual and biennial modulations in the tropical Hadley cell circulation, *Nature*, 222, 76–78, 1969.
- Reed, R. J. and Vlcek, C. L.: The annual temperature variation in the lower stratosphere, *J. Atmos. Sci.*, 26, 163–167, 1969.
- Reid, G. C. and Gage, K. S.: The tropical tropopause over western Pacific: wave driving, convection, and the annual cycle, *J. Geophys. Res.*, 101, 21233–21241, 1996.
- Seidel, D. J., Ross, R. J., Angell, J. K., and Reid, G. C.: Climatological characteristics of the tropical tropopause as revealed by radiosondes, *J. Geophys. Res.*, 106, 7857–7878, 2001.
- Simmons, A. J. and Hollingsworth, A.: Some aspects of the improvement in skill of numerical prediction, *Q. J. Roy. Meteor. Soc.*, 128, 647–677, 2002.
- Susskind, J., Barnet, C., Blaisdell, J., Iredell, L., Keita, F., Kouvaris, L., Molnar, G., and Chahine, M.: Accuracy of geophysical parameters derived from Atmospheric Infrared Sounder/Advanced Microwave Sounding Unit as a function of fractional cloud cover, *J. Geophys. Res.*, 111, D09S17, doi:10.1029/2005JD006272, 2006.
- Trenberth, K. E. and Stepaniak, D. P.: Seamless poleward atmospheric energy transports and implications for the Hadley circulation, *J. Climate*, 16, 3706–3722, 2003a.
- Trenberth, K. E. and Stepaniak, D. K.: Covariability of components of poleward atmospheric energy transports on seasonal and interannual timescales, *J. Climate*, 16, 3691–3705, 2003b.
- Trenberth, K. E., Fasullo, J., and Smith, L.: Trends and variability in column-integrated atmospheric water vapor, *Clim. Dyn.*, 24, 741–758, 2005.
- Venkat Ratnam, M., Tsuda, T., Shiotani, M., and Fujiwara, M.: New Characteristics of the Tropical Tropopause Revealed by CHAMP/GPS Measurements, *Sci. Online Lett. Atmos.*, 1, 185–188, doi:10.2151/sola.2005-048, 2005.
- Venkat Ratnam, M., Basha, G., Krishna Murthy, B. V., and Jayaraman, A.: Relative humidity distribution from SAPHIR experiment on board Megha-Tropiques satellite mission: Comparison with global radiosonde and other satellite and reanalysis datasets, *J. Geophys. Res.*, 18, 1–9, doi:10.1002/jgrd.50699, 2013.
- Venkat Ratnam, M., Pravallika, N., Ravindra Babu, S., Basha, G., Pramitha, M., and Krishna Murthy, B. V.: Assessment of GPS radiosonde descent data, *Atmos. Meas. Tech.*, 7, 1011–1025, doi:10.5194/amt-7-1011-2014, 2014a.
- Venkat Ratnam, M., Sunilkumar, S. V., Parameswaran, K., Krishna Murthy, B. V., Ramkumar, Geetha, Rajeev, K., Basha, Ghouse, Ravindra Babu, S., Muhsin, M., Mishra, Manoj Kumar, Hemanth Kumar, A., Akhil Raj, S. T., and Pramitha, M.: Tropical tropopause dynamics (TTD) campaigns over Indian region: An overview, *J. Atmos. Sol.-Terr. Phys.*, 121, 229–239, doi:10.1016/j.jastp.2014.05.007, 2014b.
- Waters, J. W., Froidevaux, L., Harwood, R. S., Jarnot, R. F., Pickert, H. M., Read, W. G., Siegel, P. H., Cofield, R. E., Filipiak, M. J., Flower, D. A., Holden, D. R., Lau, G. K., Livesey, N. J., Manney, G. L., Pumphrey, H. C., Santee, M. L., Wu, D. L., Cuddy, D. T., Lay, R. R., Loo, M. S., Perun, V. S., Schwartz, M. J., Stek, P. C., Thurstans, R. P., Boyles, M. A., Chandra, S., Chavez, M. C., Chen, G. S., Chudasama, B. V., Dodge, R., Fuller, R. A., Girard, M. A., Jiang, J. H., Jiang, Y., Knosp, B. W., Labelle, R. C., Lam, J. C., Lee, K. A., Miller, D., Oswald, J. E., Patel, N. C., Pukala, D. M., Quintero, O., Scaff, D. M., Snyder, W. V., Tope, M. C., Wagner, P. A., and Walch, M. J.: The Earth Observing System Microwave Limb Sounder (EOS MLS) on the Aura satellite, *IEEE T. Geosci. Remote*, 44, 1075–1092, doi:10.1109/TGRS.2006.873771, 2006.
- Wang, J., Carlson, D. J., Parsons, D. B., Hock, T. F., Lauritsen, D., Cole, H. L., Beierle, K., and Chamberlain, E.: Performance of operational radiosonde humidity sensors in direct comparison with a chilled mirror dew-point hygrometer and its climate implication, *Geophys. Res. Lett.*, 30, 1075–1092, doi:10.1029/2003GL016985, 2003.
- Xie, H., Nalli, N. R., Sampson, S., Wolf, W. W., Li, J., Schmit, T. J., Barnet, C. D., Joseph, E., Morris, V. R., and Yang, F.: Integration and ocean-based prelaunch validation of GOES-R Advanced Baseline Imager legacy atmospheric products, *J. Atmos. Ocean. Tech.*, 30, 1743–1756, 2013.